MNRAS **000**, 1–6 (2019) Preprint September 24, 2019 Compiled using MNRAS LATEX style file v3.0

Plasma distribution around comet 67P in the last month of the Rosetta mission

Zoltan Nemeth[1]★, A. Timar[1,2], K. Szego[1], P. Henri[3,4], R. Hajra[5]
[1]*Wigner Research Centre for Physics, Konkoly-Thege M. Rd. 29-33 Budapest, Hungary*
[2]*Eötvös Loránd University, 1117 Pázmány Péter sétány 1/A, Budapest, Hungary*
[3]*LPC2E, CNRS, Orléans, France*
[4]*Laboratoire Lagrange, OCA, CNRS, UCA, Nice, France*
[5]*National Atmospheric Research Laboratory, Gadanki 517112, India*

Accepted XXX. Received YYY; in original form ZZZ

ABSTRACT
After accompanying comet 67P/Churyumov-Gerasimenko on its journey around the Sun and observing the evolution of its induced magnetosphere throughout the comet's life-cycle, the Rosetta operations concluded at the end of September 2016 with a controlled impact on the cometary nucleus. At that time, the comet was located more than 3.8 AU from the Sun, but the data still show clear indications of a small but well developed plasma environment around the nucleus. Rosetta observed this fading cometary magnetosphere along multiple recurring elliptical orbits, which allow us to investigate its properties and spatial structure. We examined the measured electron densities along these consecutive orbits, from which we were able to determine the structure of the plasma distribution using a simple latitude and longitude dependent model.

Key words: comets: individual: 67P/Chuyumov-Gerasimenko – plasmas – methods: data analysis

1 INTRODUCTION

At 3.6 AU from the Sun, on 6 August 2014, the Rosetta spacecraft rendezvoused with comet 67P/Churyumov-Gerasimenko (67P) and began to monitor its nascent atmosphere as the comet travelled towards its perihelion. The Jupiter-family comet 67P currently has a 6.44 years long orbit around the Sun with an aphelion distance of 5.68 AU and a perihelion distance of 1.24 AU. After accompanying 67P on its journey and observing the evolution of its plasma environment throughout the comet's life-cycle for more than two years, the operations of the Rosetta orbiter concluded on 30 September 2016, at 3.8 AU from the Sun, with a controlled impact on the cometary nucleus. Throughout these two years, the ESA Rosetta mission collected a variety of measurements that provide an immense insight into cometary physics.

Nearing perihelion, the activity of comets rises, and the neutral coma expands. The large number of neutral particles are continuously ionized by photoionization, electron impact ionization and charge exchange with solar wind ions (Mendis et al. 1985; Cravens 1991; Vigren et al. 2015; Galand et al. 2016; Madanian et al. 2016; Wedlund et al. 2017; Heritier et al. 2018). During the evolution of the cometary coma of 67P, photoionization and electron impact ionization were both shown to be necessary to explain the observed electron densities over the southern, winter hemisphere while over the illuminated, northern hemisphere photoionization alone was reported to dominate the ionization processes (Galand et al. 2016; Vigren et al. 2016). After perihelion, at large heliospheric distances (2 AU), electron impact ionization dominated over photoionization and was predominant during the last 4 months of the mission on both the southern and the northern hemispheres (Heritier et al. 2018).

An early sign of the cometary plasma environment around comet 67P was observed by Nilsson et al. (2015a) through the detection of water ions in the coma on 7 August 2014. At this time, the comet was located 3.6 AU from the Sun and the comet-spacecraft distance was approximately 100 km. The newly created heavy cometary ions are accelerated by the solar wind convective electric field and are picked up by the solar wind flow. As a result of the mass loading of the solar wind with cometary ions, the solar wind suffers an energy loss and is slowed down, piled up and deflected upstream of the comet (Coates 1997; Szegö et al. 2000) although this close to the nucleus the spacecraft detected only the beginning of the mass loading process, apparent in the deflection of the solar wind ions (Behar et al. 2016).

During early activity, the high density plasma in the inner coma was investigated by Yang et al. (2016) who found that comet 67P's early plasma environment at a heliocentric distance of 3.4 AU consisted of two regions: an outer part mostly dominated by the solar wind convection electric field and an inner region of enhanced plasma density.

The evolution of the cometary ion environment was described

★ E-mail: nemeth.zoltan@wigner.mta.hu (ZN)

during early activity in 2014 as the heliocentric distance decreased from 3.6 to 2.0 AU (Nilsson et al. 2015b) as well as throughout the entirety of the mission (Nilsson et al. 2017). As the activity of the comet increased, the accelerated cometary ions became more common and reached higher energies. In April 2015, the solar wind disappeared from the vicinity of Rosetta – a solar wind cavity formed around the cometary nucleus (Behar et al. 2017). Inside the boundary called cometopause, the ion composition changes from a mixture of cometary and solar wind ions to picked-up cometary ions (Mandt et al. 2016).

In the coma of comet 67P, at relatively large heliocentric distances (2.5 AU), the ion densities fall off with the radial distance from the comet with approximately r^{-1} based on both photochemical equilibrium and transport dominant models (Galand et al. 2016; Vigren et al. 2016). Edberg et al. (2015) also reported a r^{-1} dependence of the electron densities in early 2015 within 260 km from the nucleus. These results also agree with the observations made at comet 1P/Halley during the Giotto mission (Cravens 1987).

This observed vertical cometary density profile has been confirmed down to about 3 km from the nucleus surface with the observations made on the last day of operations (30 September 2016), during the controlled descend of the Rosetta orbiter (Heritier et al. 2018), using the combined measurements of the Mutual Impedance Probe (RPC MIP) (Trotignon et al. 2007) and the Langmuir Probe (RPC LAP) (Eriksson et al. 2007) instruments of the Rosetta Plasma Consortium (Carr et al. 2007). The findings were in a close agreement with cometary vertical ionosphere models predicting a maximum in the ionospheric densities close to the surface (Vigren & Galand 2013) and a sharp decrease below this ionospheric peak (Galand et al. 2016).

Rosetta offers the unique opportunity to observe the fading cometary plasma environment in September 2016 through several similar, consecutive orbits. Our aim in this paper is to map the plasma environment around the nucleus of comet 67P through the electron densities measured by the RPC MIP experiment during the last month of the Rosetta mission. Our findings are explained and summarized by a distance, latitude and longitude dependent model of the plasma density of comet 67P.

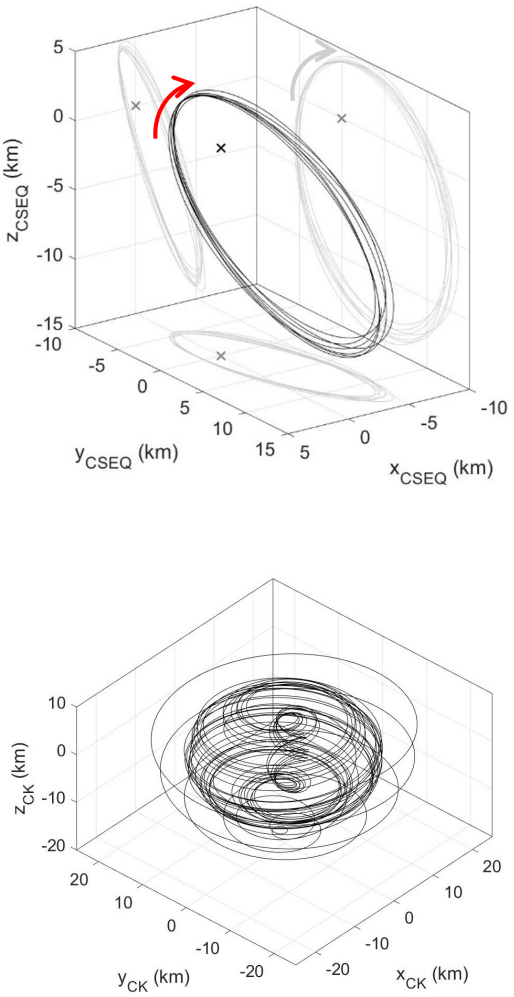

Figure 1. The trajectory of the Rosetta spacecraft in September 2016 shown in the CSEQ frame (top panel), where the +X axis points towards the Sun. The spacecraft orbited approximately in the comet's terminator plane (±5 km). The red arrow shows the direction of the spacecraft's orbit. The spacecraft's orbit in the comet-fixed (CK) frame is on the bottom panel.

2 DATA

We investigated the spatial distribution of the cometary electrons around comet 67P in September 2016, more than one year after perihelion. At that time the comet was located at 3.8 AU, with sub-solar latitudes around 18-20° on the northern hemisphere. The Rosetta spacecraft had a highly elliptical orbit at 4-17 km from the nucleus with periods of approximately 3 days (Fig. 1). The nucleus had a rotation rate of 12.4 h. During this month, Rosetta performed eight very similar, consecutive orbits around comet 67P, suitable to perform a comprehensive 3D mapping of the cometary ionosphere.

We show the electron densities measured by RPC MIP on Fig. 2. The main objective of the MIP experiment is to provide in situ the electron density and temperature in the inner coma of 67P through the measurement of the mutual impedance between two electric dipoles embedded within the plasma to be investigated (Trotignon et al. 2007). The MIP sensor is made of two receiving and two transmitting electrodes, mounted on a 1m long bar, itself mounted on a boom on the Rosetta orbiter. The instrument is capable of measuring plasma properties in two different operational modes. First, the so-called "Short Debye Length" mode (SDL), uses different combinations of a single or of the two MIP transmitters to access dense enough plasmas. Second, the so-called "Long Debye length mode" (LDL) uses the spherical probe of the LAP experiment, mounted on another boom and located 4 meters from the MIP antenna, as a monopolar transmitter. This LDL mode has been used to access lower electron densities than those accessible with the SDL mode, down to a few tens of cm^{-3}. During September 2016, MIP operated essentially in short Debye length mode, measuring densities up to thousands of cm^{-3}. The uncertainty of the measured electron density is estimated to be around 10%.

Since the length scales over which we study the density distribution is much larger than the Debye length, we assume quasi-neutrality and take the MIP electron density results as a measure of the overall plasma density. Second, since the solar wind density at 3.8 AU is much smaller than the plasma density measured by MIP around 67P, we assume these measurements correspond to the overall cometary plasma density.

The plasma density curve in Fig. 2 features clear periodicity corresponding to the orbital period of the spacecraft, but the signal is complex, not at all symmetric around the position of the closest

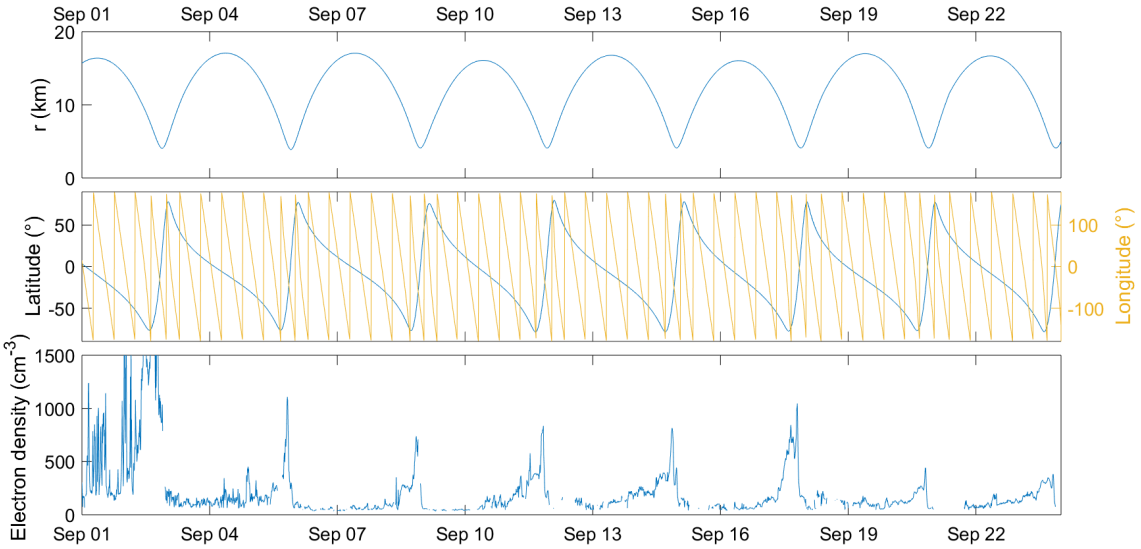

Figure 2. Rosetta's distance from the nucleus (top panel), Rosetta's latitude and longitude shown in the comet-fixed C-G_CK frame (middle panel) and the electron densities measured by MIP (bottom panel) in September 2016 before the spacecraft manoeuvred itself to collision course with the comet.

approach to the nucleus. In addition to the main recurring peak, the data also show recurring fine structure. On the top and middle panels of Fig. 2 we also show the spacecraft's radial distance from the nucleus and its latitude and longitude in the body-fixed 67P/C-G_CK coordinate frame. (The origin of the frame is located in the center of the comet, the +X axis points toward the prime meridian, the +Z axis towards the north pole while the +Y axis completes the right hand frame.)

On the first days of September 2016 a corotating interaction region (CIR) impacted on the comet and disrupted the measured electron densities (Hajra et al. 2018). In order to concentrate in this study on the unberturbed cometary plasma, we focus our investigation on the measurements from 4 September 2016 to 24 September 2016 (Fig. 2), before the spacecraft maneouvered itself to collision course with the cometary nucleus.

By investigating the position of the measurements with respect to the surface of the nucleus, we can conclude that the measured electron densities show a maximum at the southern hemisphere that falls off rapidly shortly before the spacecraft enters the northern hemisphere. On the top panel of Fig. 3, we show a projection of the trajectories onto the terminator plane in comet-centered solar equatorial (CSEQ) coordinates (the +X axis points center of mass towards the Sun, +Z axis is the component of the Sun's north pole of date orthogonal to the +X axis, the +Y axis completes the right-handed reference frame). We observe that the higher density measurements occure when the spacecraft is close to the nucleus, but the high density region is offset towards the negative z region. The bottom panel of Fig. 3 shows the data in comet fixed coordinates; the southern hemisphere clearly dominates. Although at this time the subsolar point is located at the northern hemisphere, the active regions (for cometary neutral production) were reported to be above the southern hemisphere during this period. Hansen et al. (2016) presented water distribution around the nucleus at 1.5 AU after perihelion with a maximum above the southern hemisphere, around latitudes -30°. Kramer et al. (2017) showed how the highest neutral density regions 100 km above the nucleus shift from the northern to the southern hemisphere between April 2015 and May 2016. In May 2016, the highest density regions were above latitudes around -60° and longitudes of -10°. As the main source of cometary

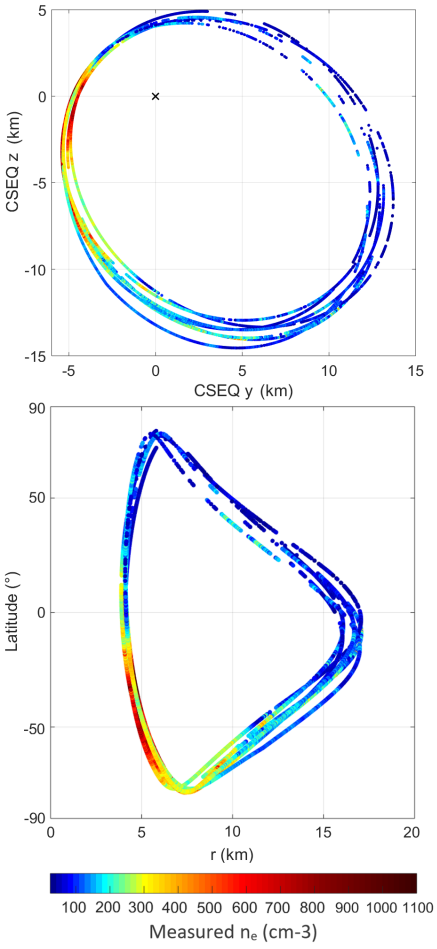

Figure 3. Electron densities measured by MIP in September 2016. On the top panel the densities are shown in the CSEQ coordinate system in the Y-Z plane. On the bottom panel the densities are shown as a function of cometocentric distance and latitude. The density values are shown according to the colour bar on the right.

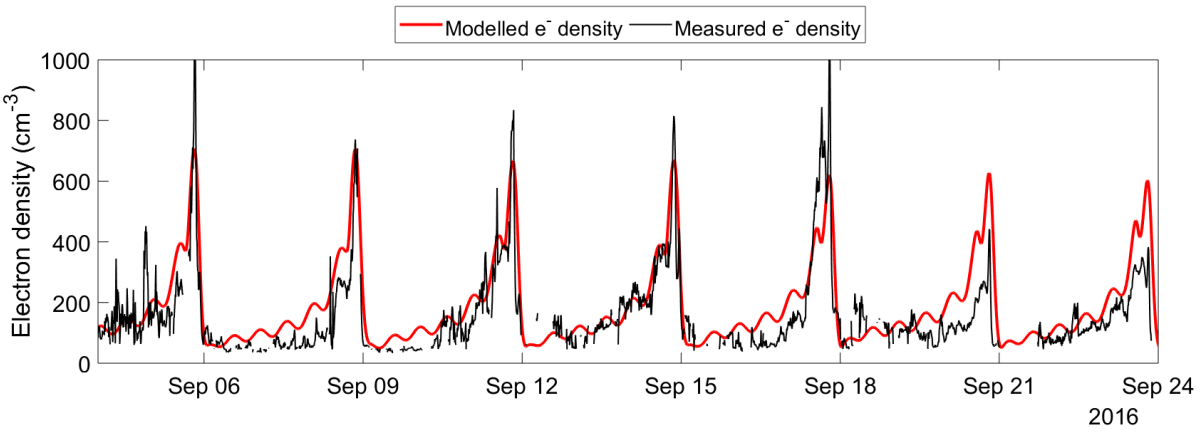

Figure 4. Modelled electron densities using a simple cometocentric distance, latitude and longitude dependent cosine function (red line) compared to the electron densities measured by MIP (black line) in September 2016.

plasma is the neutral outgassing of the nucleus, a strong correlation between the neutral and electron densities is expected.

3 MODEL

Figs. 2 and 3 show that although the radial distance plays an important role in determining the plasma density, it cannot be the sole player responsible for the observed structures. It is a reasonable hypothesis that the plasma density depends on the latitude and longitude coordinates in comet fixad frame. This hypothesis is supported by earlier results. Hansen et al. (2016) has shown that the neutral density features such angle dependence. The strongly non-spherical shape of the comet nucleus (Preusker et al. 2015; Jorda et al. 2016) and the solar-wind comet insteractions (Deca et al. 2017, 2019) can also influence the density distribution. In this section, we aim at providing a distance, latitude and longitude dependent model of the plasma density of comet 67P, which is able to reproduce the observed cometary data.

Since for these highly excentric trajectories the vicinity of closest approach is associated to a fast latitude scan, it is possible that the rapid change in latitude is responsible for the drastic variation (strongest peaks followed by very low densities in Fig. 2) found close to the nucleus. Fig. 3 qualitatively supports this hypothesis. In addition to the highly apparent slow periodicity, the data on Fig. 2 also shows fine structures (secondary and sometimes higher order peaks before the main peaks for each orbit, see e.g. Sept. 8, 11, 14 and 17 on Fig. 2). These seem to follow the rotation period of the nucleus, which suggests that the plasma distribution may be best modelled in a comet fixed coordinate system.

Thus, we modelled the 3D spatial distribution of cometary electrons around comet 67P in September 2016 in comet fixed spherical polar coordinates. We manually fitted the following simple test function to the in situ measured electron densities:

$$n(r,\theta,\varphi) = \frac{k}{r}\left(1 + a_\theta \cos\left(\theta - \theta_0\right)\right)\left(1 + a_\varphi \cos\left(\varphi - \varphi_0\right)\right). \quad (1)$$

Best fit:

$$k = 1800, \quad a_\theta = 0.83, \quad a_\varphi = 0.17, \quad \theta_0 = -90°, \quad \varphi_0 = 0°,$$

where r is the distance from the comet, k is a constant corresponding to the angle averaged mean electron density on a hypothetical spherical source surface one kilometre over the centre of the comet. The angles θ and φ are the latitude and longitude of the space-

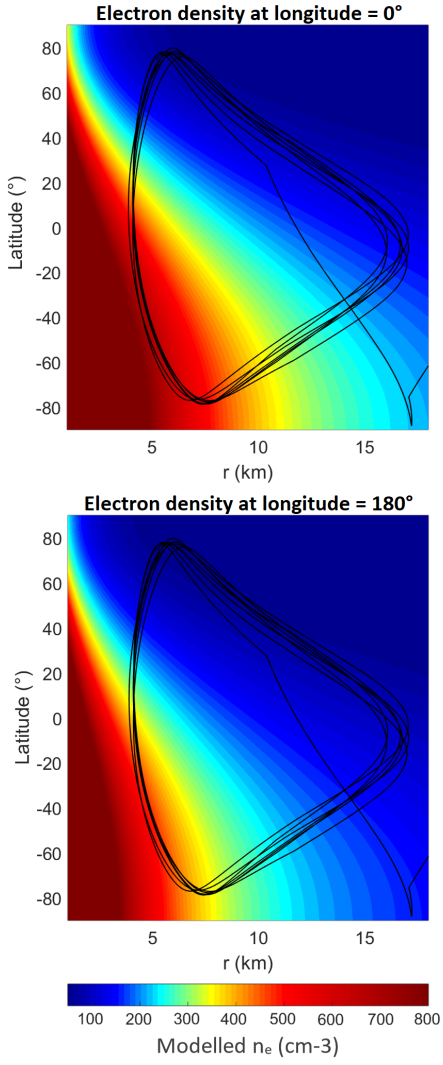

Figure 5. Modelled electron densities. The horizontal axis is the distance from the comet, the vertical axis is the latitude in the 67P/C-G_CK frame. The black line is the trajectory of the Rosetta spacecraft. The top panel shows the densities at $\lambda = 0°$, the bottom panel shows the densities at $\lambda = 180°$. Plasma density is expressed in cm^{-3} as shown in the colour bar.

craft in the comet-fixed 67P/C-G_CK frame. This is the simplest possible expression, which describes a smooth partial angle dependence for both angle coordinates together with a 1/r radial decay. The function describes the 3D cometary plasma distribution surprisingly well. The expression in the first paranthesis determines the latitudinal behaviour of the electron density. Here a_θ measures the relative weight of the latitude dependent part, θ_0 is the latitude where the electron density has a maximum. The expression in the second paranthesis determines the longitudinal behaviour of the density, where a_φ gives the relative weight of the longitudinal variations and φ_0 is the longitude where the electron density has a maximum.

We fitted the density measurements by inserting the time variation of the (r, θ, φ) coordinates of the spacecraft into this simple function. Fig. 4 shows the good aggreement between the model (red curve) and the MIP cometary plasma density in situ measurements (black). We do not expect such a simple model to account for all the short scale features observed in the measurements, which can be associated to the local plasma dynamics and/or variations in solar wind forcing. However, the model reflects the large-scale behavior very well, in particular the main periodicity, the abrupt drops after the main density peaks, and the presence of secondary peaks next to the main peaks. Moreover, it fits well both the peak widths and amplitudes. The amplitudes and sometimes the positions of the third and fourth peaks show significant deviations, which are probably due to a more complex source structure than the simple first order angle dependence we used. In our model, we assume a single smoothly varying source region, from which the majority of the ionised particles originate. The fact that this simple assumption describe the density distribution so well probably means that most of the small scale density variations are smoothed out before the gas and the plasma reaches the sampled altitudes. This does not require a collisional process, since the measured density is the sum of the contributions of all the individual sources. If the measurement is performed far enough from the sources (the distance from the surface is much larger than the source separation) then all the sources are summed up with similar geometric attenuation factors, and the result will be a smooth function reflecting the average source strength. (In contrast close to the surface, material sources closest to the spacecraft would dominate the measurements, but the 4 km minimum altitude of our orbits ensure significant averaging.)

In agreement with previous results based on measurements from earlier phases of the comets lifetime (Galand et al. 2016; Edberg et al. 2015; Vigren et al. 2016), the electron density falls off with approximately r^{-1} in the fading coma of comet 67P. This r^{-1} dependence of the electron density is a remarkably persistent feature of the cometary environment.

The electron density features a maximum in the southern hemisphere, the best fit to the measured MIP data is achieved when we set the location of the maximum of the density around $\theta_0 = -90$, although <5° deviation from this value gives similar fit qualities. This result agrees well with the findings of investigations of the neutral density after perihelion (Hansen et al. 2016; Kramer et al. 2017) that found an active southern hemisphere and showed the separation of the sub-solar point and the highest density areas above the comet.

Kramer et al. (2017) reported that in May 2016 the neutral densities had a maximum above longitudes around -10°. In agreement with this we assumed an electron density maximum at $\varphi_0 = 0$ for our model. Values between -20° and +20° give similar results.

This study shows that the latitude plays a very important role in the density distribution: the high $a_\theta = 0.83$ latitudinal modulation amplitude means that the density over the north pole is only 9%

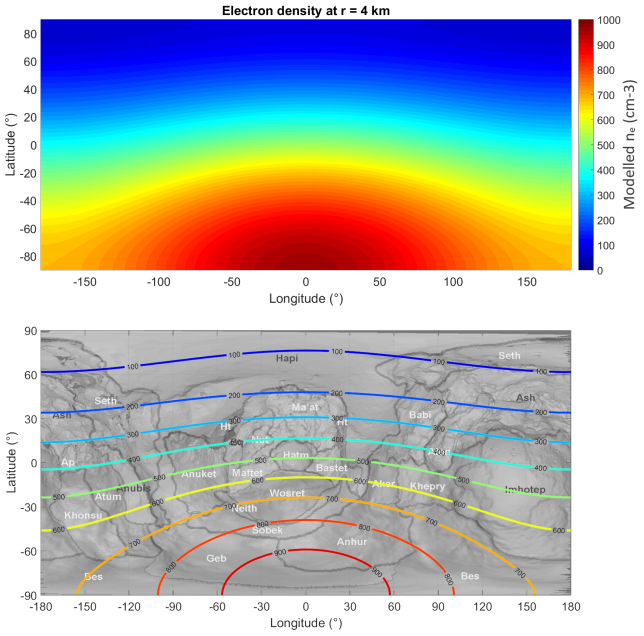

Figure 6. Modelled electron densities. The horizontal axis is the distance from the comet, the vertical axis is the latitude in the 67P/C-G_CK frame. The black line is the trajectory of the Rosetta spacecraft. The figure in the left panel shows the densities at , the right panel shows the densities at. The plasma density is expressed in cm^{-3} as shown in the colour bar.

of the density over the south pole, the ratio of the two values is $(1 - 0.83)/(1 + 0.83) \approx 0.09$. In contrast, the longitudinal position influences the density only slightly, with an $a_\varphi = 0.17$modulation amplitude. Thus the minimum in longitude is 71% of the maximum since $(1 - 0.17)/(1 + 0.17) \approx 0.71$.

A radial distance - latitude map of the model density distribution is shown in Fig. 5, to be compared to the right panel of Fig. 3. The model explains the cometary plasma densities measured along the Rosetta orbiter trajectories very well. Fig. 6 is a longitude-latitude map of the electron density 4km over the centre of the nucleus. This is the minimum altitude sampled by these orbits, but according to Heritier et al. (2017), this altitude also coincide with the peak ionospheric density. The bottom panel projects the density contours onto a map showing surface features and regions of 67P.

These maps show the plasma distribution in comet fixed coordinates. Since at this time of the mission both the neutral flow and the plasma is tenuous, the bulk motion of plasma particles points radially outwards from the cometary nucleus in inertial frame. This means that in comet fixed coordinates they move along slightly bent trajectories. Since close to the nucleus the radial flow speed is much larger (~500-1000 m/s, (Hansen et al. 2016)) than the apparent tangential speed (~2 m/s at 15km from the comet) in the comet fixed frame, this effect does not change the picture described above; close to the nucleus the plasma motion can be assumed to be approximately radial in comet fixed frame as well. In the 4-15 km radial range of our study we see a plasma cloud radially expanding with respect to the comet and preserving the original latitude-longitude distribution of the source surface.

4 CONCLUSIONS

Near the end of the Rosetta orbiter operations, although comet 67P was more than 3.8 AU from the Sun, in situ measurements still show clear signs of a small, fading cometary plasma environment. During the last month of the Rosetta operations, in September 2016, the spacecraft moved along a periodic, recurrent orbit that made it possible to study the 3D spatial distribution of the plasma density near the nucleus. In this paper, we derived a simple and therefore useful model to explain the plasma density distribution in the coma of comet 67P in September 2016.

Based on in situ MIP electron density measurements we defined a simple distance, latitude and longitude dependent first order cosine function to model the 3D spatial distribution of the cometary plasma. This 3D cometary plasma density distribution model reproduced the Rosetta observations remarkably well. The model reflects the observed structures, in particular the main periodicity, the abrupt drops after the main peaks, even the presence of secondary peaks next to the main peaks; it fits well the peak widths as well as the amplitudes.

The plasma density distribution show a strong latitudinal dependence: the plasma density is highest above the southern hemisphere, which is consistent with the neutral density observations after the comet's perihelion passage (Hansen et al. 2016; Kramer et al. 2017). Indeed, the southern, nightside hemisphere produces more plasma than the sunlit northern hemisphere – mostly due to the higher neutral outgassing rates. Our model shows that the plasma density can be described well by assuming only a single plasma source in longitudes around 0°. This also correlates with the findings of Kramer et al. (2017) who found that in May 2016 the neutral densities had a maximum above longitudes around -10°.

ACKNOWLEDGEMENTS

Rosetta is an ESA mission with contributions from its member states and NASA. We thank the Rosetta Mission Team, SGS, and RMOC for their outstanding efforts in making this mission possible. The work of Z. N. was supported by the János Bolyai Research Scolarship of the Hungarian Academy of Sciences. The work at LPC2E/CNRS was supported by CNES and by ANR under the financial agreement ANR-15-CE31-0009-01. The work of R. H. is funded by the Science & Engineering Research Board (SERB), a statutory body of the Department of Science & Technology(DST), Government of India through Ramanujan Fellowship at NARL.

References

Behar E., Nilsson H., Wieser G. S., Nemeth Z., Broiles T. W., Richter I., 2016, Geophys. Res. Lett., 43, 1411
Behar E., Nilsson H., Alho M., Goetz C., Tsurutani B., 2017, Monthly Notices of the Royal Astronomical Society, 469, S396
Carr C., et al., 2007, Space Science Reviews, 128, 629
Coates A., 1997, Advances in Space Research, 20, 255
Cravens T., 1987, Advances in Space Research, 7, 147
Cravens T. E., 1991, International Astronomical Union Colloquium, 116, 1211
Deca J., Divin A., Henri P., Eriksson A., Markidis S., Olshevsky V., Horányi M., 2017, Physical Review Letters, 118, 205101
Deca J., Henri P., Divin A., Eriksson A., Galand M., Beth A., Ostaszewski K., Horányi M., 2019, Physical Review Letters, 123, 055101
Edberg N. J. T., et al., 2015, Geophysical Research Letters, 42, 4263
Eriksson A. I., et al., 2007, Space Science Reviews, 128, 729
Galand M., et al., 2016, Monthly Notices of the Royal Astronomical Society, 462, S331
Hajra R., et al., 2018, Monthly Notices of the Royal Astronomical Society, 480, 4544
Hansen K. C., et al., 2016, Monthly Notices of the Royal Astronomical Society, 462, S491
Heritier K. L., et al., 2017, Monthly Notices of the Royal Astronomical Society, 469, S118
Heritier K. L., et al., 2018, A&A, 618, A77
Jorda L., et al., 2016, Icarus, 277, 257
Kramer T., Läuter M., Rubin M., Altwegg K., 2017, Monthly Notices of the Royal Astronomical Society, 469, S20
Madanian H., et al., 2016, Journal of Geophysical Research: Space Physics, 121, 5815
Mandt K. E., et al., 2016, Monthly Notices of the Royal Astronomical Society, 462, S9
Mendis D. A., Houpis H. L. F., Marconi M. L., 1985, Fundamentals of Cosmic Physics, 10, 380
Nilsson H., et al., 2015a, Science, 347, aaa0571
Nilsson H., et al., 2015b, A&A, 583, A20
Nilsson H., et al., 2017, Monthly Notices of the Royal Astronomical Society, 469, S252
Preusker F., et al., 2015, A&A, 583, A33
Szegö K., et al., 2000, Space Sci. Rev., 94, 429
Trotignon J. G., et al., 2007, Space Science Reviews, 128, 713
Vigren E., Galand M., 2013, The Astrophysical Journal, 772, 33
Vigren E., Galand M., Eriksson A. I., Edberg N. J. T., Odelstad E., Schwartz S. J., 2015, The Astrophysical Journal, 812, 54
Vigren E., et al., 2016, The Astronomical Journal, 152, 59
Wedlund C. S., et al., 2017, A&A, 604, A73
Yang L., Paulsson J. J. P., Simon Wedlund C., Odelstad E., Edberg N. J. T., Koenders C., Eriksson A. I., Miloch W. J., 2016, Monthly Notices of the Royal Astronomical Society, 462, S33

This paper has been typeset from a TEX/LATEX file prepared by the author.